

# Answer Set Networks: Casting Answer Set Programming into Deep Learning

Arseny Skryagin<sup>\*1</sup>, Daniel Ochs<sup>\*1</sup>, Philipp Deibert<sup>1</sup>, Simon Kohaut<sup>1</sup>  
Devendra Singh Dhami<sup>2</sup>, Kristian Kersting<sup>1,3,4</sup>

<sup>1</sup>AI & Machine Learning Group, CS Dept., TU Darmstadt

<sup>2</sup>Uncertainty in AI Group, Dept. of Mathematics and CS, TU Eindhoven

<sup>3</sup>Hessian Center for AI (hessian.AI)

<sup>4</sup>German Research Center for AI (DFKI)  
{first.last}@cs.tu-darmstadt.de

## Abstract

Although Answer Set Programming (ASP) allows constraining neural-symbolic (NeSy) systems, its employment is hindered by the prohibitive costs of computing stable models and the CPU-bound nature of state-of-the-art solvers. To this end, we propose Answer Set Networks (ASN), a NeSy solver. Based on Graph Neural Networks (GNN), ASNs are a scalable approach to ASP-based Deep Probabilistic Logic Programming (DPPL). Specifically, we show how to translate ASPs into ASNs and demonstrate how ASNs can efficiently solve the encoded problem by leveraging GPU’s batching and parallelization capabilities. Our experimental evaluations demonstrate that ASNs outperform state-of-the-art CPU-bound NeSy systems on multiple tasks. Simultaneously, we make the following two contributions based on the strengths of ASNs. Namely, we are the first to show the fine-tuning of Large Language Models (LLM) with DPPLs, employing ASNs to guide the training with logic. Further, we show the “constitutional navigation” of drones, i.e., encoding public aviation laws in an ASN for routing Unmanned Aerial Vehicles in uncertain environments.

## Introduction

The paradigm of modeling an application-specific problem in a logical language to then apply a general solving approach has a long-standing history. To this end, Answer set programming (ASP), being a modern, non-monotonic reasoning framework based on stable model semantics, has experienced rising interest in NeSy inference systems. In this vein, recent NeSy AI pipelines (Skryagin et al. 2023, 2022; Yang, Ishay, and Lee 2020) have relied on a foundation of ASP for providing a declarative modeling language of rules and background knowledge. Although conflict-driven, state-of-the-art solvers like clingo (Gebser et al. 2011) and DLV (Alviano et al. 2017) continually improve, the computational cost of today’s ASP solvers remains an open issue to the real-world application of NeSy systems.

Many deep probabilistic logic programming languages utilize such CPU-based solving frameworks. Lately, languages such as SLASH and NeurASP using ASP or Deep-ProbLog (Manhaeve et al. 2018) and Scallop (Huang et al. 2021) using Sentential Decision Diagram (Darwiche 2011)

rely on neural computations on the GPU and symbolic computations on the CPU. SLASH, relying on clingo as the backbone, uses *multithreading* of the CPU to scale. And, SAME provides the speed-up based on *top-k%*. Although these are great advancements for scaling NeSy AI, the gap in computational speed to support seamless communication with deep learning models remains substantial to this day. This becomes even more prevalent in NeSy systems like Alpha Geometry (Trinh et al. 2024). There, 10k CPU cores were used to train a model to reach the silver medal level in geometry at the math Olympiads.

Following this trend, the question of how to integrate these pipelines tightly with modern GPUs is more urgent than ever. For example, large machine learning models for natural language and vision tasks have dramatically risen in popularity and public awareness. Widely known, their success is greatly supported by their underlying architectures’ ability to distribute work on many-core systems with ease. Thus, translating the task of solving ASP-based modeling into a neural framework that leverages modern hardware acceleration to the same level can be seen as a key to applying NeSy systems in real-world applications.

Usually, in state-of-the-art solvers, the search for the solutions, i.e., the stable models, of a program  $\Pi$  among all interpretations follows a binary tree. That is, branches of the tree correspond to (partial) assignments of truth values to the program’s atoms (partial interpretations). Further, alternating between decision and propagation phases generates the searched stable models of the ASP. However, recent research has proposed alternative approaches based on the propagation of truth values within a graph. Such graph-based Answer Set Programming solver systems (Li 2021) are based on *Dependency Graphs* as a basis. The advantage of this explicit representation of atoms and literals as graph nodes is the uniform representation of stable models and preservation of causal relationships, meaning each atom is justified in a particular stable model. Hence, the usual heuristics inherited from SAT solvers are avoided, i.e., the solving procedure is transparent.

Along this line of research, we investigate a GNN-based representation of ASPs and the search for stable models. More precisely, we present the novel NeSy ASP-solver *An-*

<sup>\*</sup>These authors contributed equally.

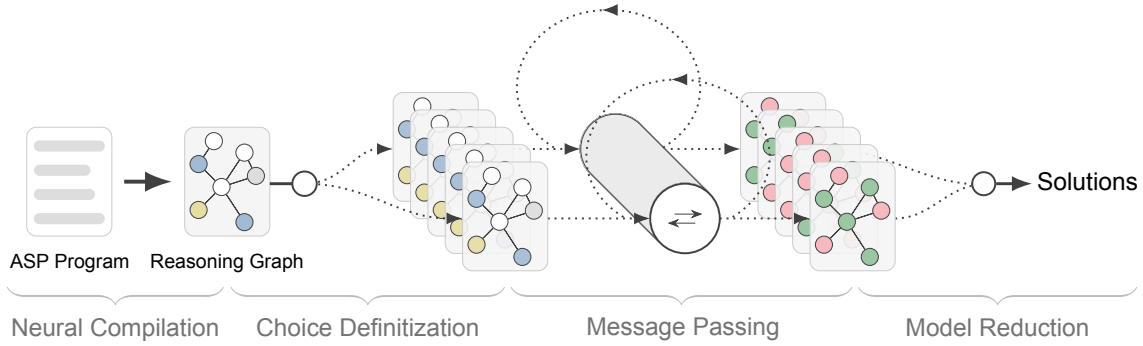


Figure 1: **ASN solving process:** ASN takes a grounded ASP program as input and translates it into an equivalent Reasoning Graph via neural compilation. The RG instances representing all possible choice selections are constructed in the definitization stage, to be iteratively solved in parallel using message passing. Finally, the resulting models are reduced to yield the ASP’s stable models.

*swer Set Networks (ASN)*<sup>12</sup>. Within ASNs, we translate ASPs into equivalent Graph Neural Network (GNN) by introducing Reasoning Graphs (RG) as illustrated in Fig. 1. By introducing a set of building blocks as laid out in Fig. 2, each element of an ASP program finds its respective representation within an RG. ASN is motivated by grASP (Li 2021) to encode relationships and atoms as edges and nodes, respectively, to obtain stable models in a parallelizable way.

ASN as a NeSy solver of ASP problems, utilizes forward reasoning: First, they generate interpretations, i.e., labelings of the ground atoms. Second, they filter through them to yield all the ASP’s stable models. ASN’s motivation for the generation of interpretations is rooted in flow-networks. Specifically, the ASN propagates truth values starting at a “source” node  $\top$ , from which the truth information can flow through the ASN until it reaches the “sink” node  $\perp$ . Hence, ASN can check whether an interpretation is valid or not according to the ASP.

In summary, we make the following contributions:

- We introduce Answer Set Networks, a novel ASP solver tailored towards scaling NeSy AI on many-core systems.
- We demonstrate the compilation of ASP programs into Reasoning Graphs and show how to obtain the respective stable models through message passing and model reduction.

Our claims of ASNs outperforming state-of-the-art solutions in NeSy AI are substantiated in an exhaustive evaluation. First, we demonstrate how ASN allows for *abductive fine-tuning* of Large Language Models (LLMs), alleviating the *Reversal Curse* (Berglund et al. 2024). Second, ASN’s raw performance benefits on the probabilistic mission design task for Unmanned Aerial Vehicles (UAV) (Kohaut et al. 2023), showing three orders of magnitude faster inference than the baseline. Finally, we investigate our contribution in detail in an ablation study showing empirical results on MNIST-Addition (Manhaeve et al. 2018).

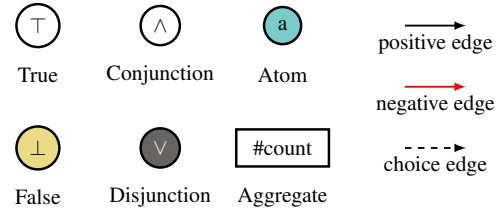


Figure 2: **Building Blocks of any Reasoning Graph:** We depict nine distinct elements to compile any ground ASP program into an RG.

In the following, we introduce ASNs and how every element of the ASP-Core-2 language (Calimeri et al. 2020) can, by our neural-compilation process, be translated into an equivalent RG. Afterward, we explain how truth value propagation via message passing is used to obtain the stable models from the RG.

### Casting Answer Set Programs into GNNs

Here, we show how the ASP-Core-2 (Calimeri et al. 2020) language is encoded and solved in the form of the RG. ASN expects a grounded, i.e., variable-free and tight (acyclic) ASP-program,  $\Pi$ . Fig. 1 gives the overview of the ASN-pipeline, from a grounded ASP-program to *stable models* (SM). The pipeline consists of four steps, which we will describe in separate subsections.

### Reasoning Graph

Let  $\mathcal{G} = (\mathcal{V}, \mathcal{E})$  be a *heterogeneous graph*, with a set of *nodes*  $\mathcal{V}$  and a set of *edges*  $\mathcal{E} \subseteq \mathcal{V} \times \mathcal{V}$ . Further, all nodes  $v \in \mathcal{V}$  and edges  $e \in \mathcal{E}$  have an associated *type*  $\tau_v \in \mathcal{A}$  and  $\tau_e \in \mathcal{R}$ , where  $\mathcal{A}$  is the set of node types and  $\mathcal{R} \subseteq \mathcal{A} \times \mathcal{A}$  is the set of edge types, respectively <sup>2</sup>. The tuple  $(\mathcal{A}, \mathcal{R})$  is called the *network schema* of  $\mathcal{G}$  and is itself a graph representing the node types and the possible relations between them. A

<sup>1</sup>The plural signalizes that for solving, a stack of graphs is used.

<sup>2</sup>Code <https://github.com/ml-research/answersetnetworks/>

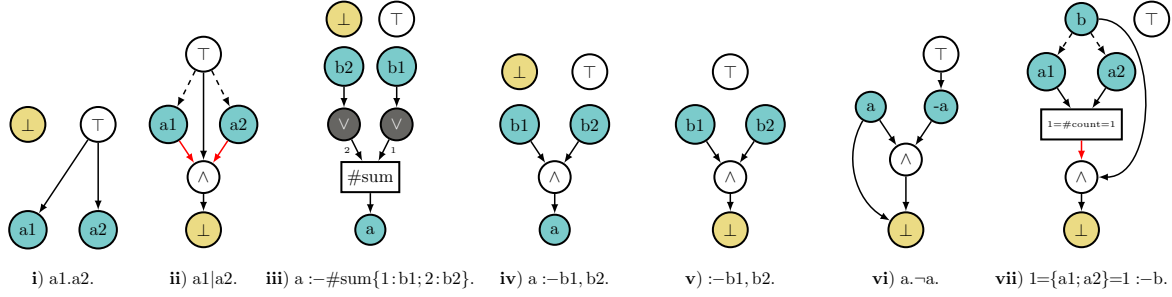


Figure 3: **Neural Compilation of ASP-Core-2 Elements into RG:** For each element of the ASP syntax, we generate the equivalent *Reasoning Graph* (RG) representation encoded as GNN. The graphs are generated automatically from grounded ASP-programs. From left to right, some building-blocks of the overall RG are: **i) facts**, **ii) disjunctive facts**, **iii) aggregate literal**, **iv) rule**, **v) constraint**, **vi) classical negation**, **vii) choice rule**.

*reasoning graph* is a heterogeneous graph where

$$\mathcal{A} := \underbrace{\{A_{\wedge}, A_{\vee}\}}_{\mathcal{A}_{\text{logical}}} \cup \underbrace{\{A_{\text{count}}, A_{\text{sum}}, A_{\text{min}}, A_{\text{max}}\}}_{\mathcal{A}_{\text{aggr}}} \quad (1)$$

$$\mathcal{R} := \underbrace{(\mathcal{A} \times \mathcal{A}_{\text{logical}})}_{\mathcal{R}_{\text{logical}}} \cup \underbrace{(\mathcal{A}_{\text{logical}} \times \mathcal{A}_{\text{aggr}})}_{\mathcal{R}_{\text{aggr}}} \quad (2)$$

An RG is constructed from a ground ASP program, where the nodes represent logical constructs – namely classical atoms, aggregate literals, as well as conjunctions and disjunctions of the former two – and the edges indicate rules for constructs to be true as defined by the semantics of the specified program  $\Pi$ .

### Neural Compilation

We introduce the process of neural compilation into an RG for each element of the ASP syntax. Fig. 2 visualizes all basic elements of our RGs. Positive edges are shown in black, while red is used for negative ones. Additionally, edges are annotated with their corresponding edge weights. Dashed edges are parts of either disjunctive or choice-rules to indicate that they may or may not be active. There are three categories in the ASP syntax: atoms, literals, and statements, which we will consider separately.

**Atoms** Each RG has two special atom nodes,  $\top$  (true) and  $\perp$  (false), which, if connected to each other through other nodes, indicate true and false statements, respectively.  $\top$  is always part of any valid interpretation and propagates truth values. Facts, which are by design true, are always connected to the  $\top$  node via an incoming edge (Fig. 3 **i**). The  $\perp$  node is used to indicate contradictions, model constraints, and ensures interpretation consistency. Therefore, its purpose is to indicate the satisfiability of an interpretation  $I$  or formally  $I \models \Pi$ . We limit  $\top$  to have no incoming edges and  $\perp$  to have no outgoing edges, calling them *source* and *sink* nodes. Apart from facts, other program atoms are defined through statements. For an atom to be true, at least one rule defining the atom, we express their combination through a disjunction. Each unique classical atom is represented as an

individual disjunction node. Note that predicate atoms and their negations are encoded separately.

**Literals** Due to the program being already grounded, we know if a built-in literal evaluates to true or false. For conjunctions, true built-in literals can be ignored safely while making sure that false ones cannot be satisfied. In the latter case, the conjunction can be treated as false as well. For disjunctions, we change the course by ignoring false built-in literals and setting any to true if it evaluates to true itself. Thus, during neural-compilation, built-in literals are handled implicitly.

Next, we consider an aggregate literal of the form  $\beta_{v,l} \diamond_{v,l} f \{T_i : C_i\} \diamond_{v,r} \beta_{v,r}$ . Herein, we consider *aggregate function*  $f \in \{\#count, \#sum, \#min, \#max\}$ , *relational operators*  $\diamond_{v,l/r} \in \{=, \neq, <, >, \leq, \geq\}$ , *terms*  $\beta_{v,l/r}$ , *aggregate elements*  $T_i : C_i$  with  $T_i$  and  $C_i$  being sequences of terms and negation-as-failure (NAF) literals respectively. See Fig. 3 **iii**) for an example of  $\#sum$  aggregate. Each unique term  $T_i$  is aggregated only once if satisfied but may be satisfied by one or more NAF-literals  $C_i$ . Let  $T = \{T_1, \dots, T_k\}$  be the set of terms appearing in the aggregate elements, and  $C(T_i) = \{C_j | T_i : C_i \in \{T_1 : C_1, \dots, T_k : C_k\}\}$  the set of all conditions defining each  $T_i \in T$ . A term  $T_i \in T$  is aggregated if and only if some NAF-literal  $C_j \in C(T_i)$  is satisfied. This can be rewritten as a disjunction of the different NAF-literals,  $\bigvee_{C \in C(T_i)} C$ . It is then connected to an aggregate node  $\#aggr$  with edge weight  $f(\{T_i\})$ . Both, *left-guard*  $\beta_{v,l} \diamond_{v,l}$  and *right-guard*  $\diamond_{v,r} \beta_{v,r}$  are encoded in the aggregate node.

**Statements** A rule has the general form  $H :- B$ . with the head,  $H$  and the body,  $B$ . Semantically, it is equivalent to a conjunction of the body literals. This conjunction node combines the body literals via negative or positive edges, depending on whether the corresponding literal is default-negated or not. For facts, the body consists of  $\top$ .

In compiling  $a :- b_1, \dots, b_n$ , the conjunction node is directly connected to the node representing the *consequent atom*  $a$ , Fig. 3 **iv**). *Constraints*,  $a :- b_1, \dots, b_n$ , are treated the same way assuming the head atom  $\perp$ , signifying an invalid interpretation if the body is true, Fig. 3 **v**).

For *disjunctive rules*,  $a_1 | \dots | a_m :- b_1, \dots, b_n$ , the conjunction node is connected to all consequent atoms  $a_1, \dots, a_m$  and each edge representing a choice to be made. A subset of the edges may be removed in advance to represent a corresponding choice. Further, at least one of the consequent atoms needs to be true if the body of the rule is true. Consequentially, we add an appropriate constraint,

$$:-b_1, \dots, b_n, \mathbf{not} a_1, \dots, \mathbf{not} a_m. \quad (3)$$

rendering the current configuration invalid if the body holds but none of the consequent atoms. E.g., Fig. 3 ii) with an empty body.

The *choice rule* is encoded directly: Head atoms may have extra conditions that must be fulfilled in addition to the body. The conjunction node, representing the body, can, in this case, not be directly connected to the consequent atoms but needs to be combined with the disjunctions, representing that some condition for the individual head atoms is fulfilled. Additionally, it must be ensured that if the body is true, so are a valid number of head atoms as defined by the guards of the choice. Thus, we add a similar to Eq. 3 constraint.

*Weak constraints*,  $:\sim b_1, \dots, b_n.[w@l, t_1, \dots, t_m]$  (with terms  $w, l, t_1, \dots, t_m, m > 0, w$  for weight and  $l$  for level), are ranking the resulting stable models and consequentially handled by the solver after computing all solutions without encoding into RG.

*Classical negation* can be regarded as syntactic sugar, where  $\neg a$  is treated as a separate unique predicate symbol while keeping the same semantics. To ensure consistency of a program,  $\Pi$  both  $a$  and  $\neg a$  cannot be part of the same model. This requirement is encoded as the constraint  $:-a, \neg a.$  with  $\forall a, \neg a \in \Pi$ , and is shown in Fig. 3 vi).

*Queries* in ASP are encoded as constraints and can be incorporated as such in the RG. The key insight is that the majority of the program (up to the queries) is identical in all cases, and most of RG can be shared. To separate the satisfiability values (i.e., the node values of the sink node) for different queries, we encode them using distinct sink nodes  $\perp_{Q_1}, \dots, \perp_{Q_n}$ . The global sink node is then connected to these special sink nodes to pass along the satisfiability values of the main part of the program.

### Choice definitization

An RG may represent a program that contains disjunctive and choice rules. We consider an example program containing the single rule  $a_1 | a_2 :- B.$  with  $B$  being some sequence of NAF-literals. This example can be represented by the set of programs  $\{\{a_1 :- B.\}, \{a_2 :- B.\}, \{a_1 :- B., a_2 :- B.\}\}$ , which we will call *program definitives* (or *definitives* for short). Each answer set of the original program consists of the *program definitives*, making a different possible choice definite, transforming the original one into a normal program with a deterministic cause-effect relationship between classical atoms. The RG representing these definitives can be directly constructed from a copy of the RG representing the original program, disabling (removing) the appropriate edges connecting the body to the non-selected consequent head atoms. For programs containing multiple disjunctive, choice, and NPP-rules, all combinations of their respective

variants need to be considered; Which, in turn, yields easy parallelization of RG.

### Message-Passing

Given a starting configuration of nodes that are considered true, we propagate truth values through the graph with the goal of computing the (stable) models of the program. Thus, we associate with every node  $v \in V$  a boolean *node value*  $h_{v,t} \in \{0, 1\}$  at a time step  $t \in \mathbb{N}$ . Except for  $\top$ , all nodes are initially set to false (0) at  $t = 0$ .

Aggregate nodes  $v \in \mathcal{V}, \tau_v \in \mathcal{R}_{\text{aggr}}$  additionally have terms  $\beta_{v,l}, \beta_{v,r} \in \mathbb{N}$  and relation operators  $\diamond_{v,l}, \diamond_{v,r} \in \{=, \neq, <, >, \leq, \geq\}$  linked to them, representing the guards of the corresponding aggregate. Furthermore, each edge  $e \in \mathcal{E}$  has a *weight*

$$w_e \in \begin{cases} \{-1, 1\} & \text{if } e \in \mathcal{E}_{\text{logical}}, \\ \mathcal{U} & \text{if } e \in \mathcal{E}_{\text{aggr}}. \end{cases} \quad (4)$$

We can then define the node values for the next time step recursively as  $h_{v,t+1} =$

$$\begin{cases} \bigwedge_{\substack{e=(u,v) \in \mathcal{E}, \\ w_e=1}} h_{u,t} \wedge \bigwedge_{\substack{e=(u,v) \in \mathcal{E}, \\ w_e=-1}} \neg h_{u,t} & \text{if } \tau_v = A_{\wedge}, \\ \bigvee_{\substack{e=(u,v) \in \mathcal{E}, \\ w_e=1}} h_{u,t} \vee \bigvee_{\substack{e=(u,v) \in \mathcal{E}, \\ w_e=-1}} \neg h_{u,t} & \text{if } \tau_v = A_{\vee}, \\ g_{v,l} | \mathcal{E}_t^{\text{in}, \top}(v) | g_{v,r} & \text{if } \tau_v = A_{\text{count}}, \\ g_{v,l} \sum_{e \in \mathcal{E}_t^{\text{in}, \top}(v)} w(e) g_{v,r} & \text{if } \tau_v = A_{\text{sum}}, \\ g_{v,l} \min^{\preceq}(\mathcal{W}_t^{\text{in}, \top}(v) \cup \{\#\text{sup}\}) g_{v,e} & \text{if } \tau_v = A_{\text{min}}, \\ g_{v,l} \max^{\preceq}(\mathcal{W}_t^{\text{in}, \top}(v) \cup \{\#\text{inf}\}) g_{v,r} & \text{if } \tau_v = A_{\text{max}}. \end{cases} \quad (5)$$

where  $g_{v,l/r} := \beta_{v,l/r} \diamond_{v,l/r}$ ,  $\mathcal{E}_t^{\text{in}, \top}(v) := \{e | e = (u, v) \in \mathcal{E}, h_{u,t} = 1\}$  is the set of incoming edges of  $v \in \mathcal{V}$  whose source nodes are 1 (true) at time step  $t \in \mathbb{N}$  and  $\mathcal{W}_t^{\text{in}, \top}(v) := \{w_e | e \in \mathcal{E}_t^{\text{in}, \top}(v)\}$  the set of corresponding edge weights.

Updates at the time step  $t+1$  can be understood in the following way. Logical nodes  $v \in \mathcal{V}_{\text{logical}}$  take on the value of the conjunction or disjunction of their incoming neighbors' values, where the edge weight determines whether the corresponding node value is included positively or negatively. We therefore call an edge  $e \in \mathcal{E}_{\text{logical}}$  *positive* if  $w_e = 1$  and *negative* otherwise. For aggregate nodes,  $v \in \mathcal{V}_{\text{aggr}}$ , the edge weights of incoming edges signify the values to be aggregated but are only included if the source node is considered true. The node value of an aggregate node is then determined by checking the guards of the aggregated value. For  $\#\text{min}$  and  $\#\text{max}$  aggregates, we include the default value for empty sets. I.e.,  $\#\text{sup}$  and  $\#\text{inf}$  for an infinite  $T$  and swapping both otherwise.

### Model Reduction

After message passing, the graphs represent interpretations, as indicated by the truth values of the nodes representing

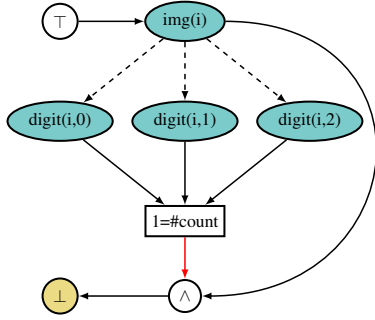


Figure 4: **Example of Neural-Probabilistic Predicate:**  $img(i). \#npp(digit(i), [0, 1, 2]) :- img(i).$

classical atoms. If  $\perp$  is true for some graph instance, then the corresponding interpretation is not a model. However, the interpretation does not equate to a stable model of the original program. Accurately, ASP’s models are minimal w.r.t. inclusion. Thus, we filter all the program’s models to obtain the minimal one. This can be done efficiently in a batch-wise manner using logical bit-wise operators. Let  $I_1, I_2 \subseteq A = \{a_1, \dots, a_n\} \subseteq \mathcal{B}_{\Pi}$  be two interpretations over some finite subset of Herbrand base  $\mathcal{B}_{\Pi}$ . Further, let  $m_1, m_2 \in \{0, 1\}^n$  be vectors representing the truth values of the corresponding interpretations with the components  $m_{i_j} = 1$  if and only if  $a_j \in I_i$ . We have  $m_1 \otimes m_2 =$

$$\begin{cases} m_1 & \text{if } I_1 \subseteq I_2, \\ m_2 & \text{if } I_1 \supseteq I_2, \\ m \in \{0, 1\}^n, m_1 \neq m \neq m_2 & \text{else.} \end{cases} \quad (6)$$

where  $\otimes$  represents element-wise logical conjunction (or multiplication). For a set of interpretations  $\{I_1, \dots, I_k\} \subseteq A$  with corresponding 0-1-vectors  $m_1, \dots, m_k$ , the set of answer sets can be computed as AS ( $\Pi$ ) =

$$\{I_i | i \in \{1, \dots, n\} : m_i \otimes m_j \neq m_i, \forall j = i + 1, \dots, n\} \quad (7)$$

## Neural Probabilistic Predicates

We have now seen how to extract stable models with ASN. To use ASN for NeSy AI, we can use *Neural-Probabilistic Predicates* (NPP) from SLASH (Skryagin et al. 2022, 2023) within ASN:

$$\#npp(h(x), [v_1, \dots, v_n]) \leftarrow Body \quad (8)$$

$npp$  is a reserved term labeling the NPP,  $h$  a symbolic name of either a probabilistic circuit (Choi, Vergari, and Van den Broeck 2020), neural network or a joint of both. Fig. 4 displays an example of an NPP. With NPPs, ASN allows for neural probabilistic programming and, simultaneously, probabilistic programming. For a thorough introduction to the SLASH semantics, we refer to (Skryagin et al. 2023). In general, SLASH can be seen as a superclass of ASP.

## Experiments

In this section, we show how ASN scales DPPLs with ASP as backbone in various tasks by answering the following questions:

- Q1 Which advantages offers **LLM fine-tuning with ASN** for the Reversal Curse (Berglund et al. 2024)?
- Q2 Can ASN scale the task of **mission design for unmanned aerial vehicles**, as proposed by (Kohaut et al. 2023), to cover Paris and its immediate surroundings?
- Q3 How competitive can ASN be in a NeSy setting such as **MNIST-Addition** (Manhaeve et al. 2018)?

Further, throughout the experiments, we refer to **ASN** as SLASH using ASN as ASP-solver and with **SLASH** (Skryagin et al. 2022) the same DPPL but using clingo as solver.

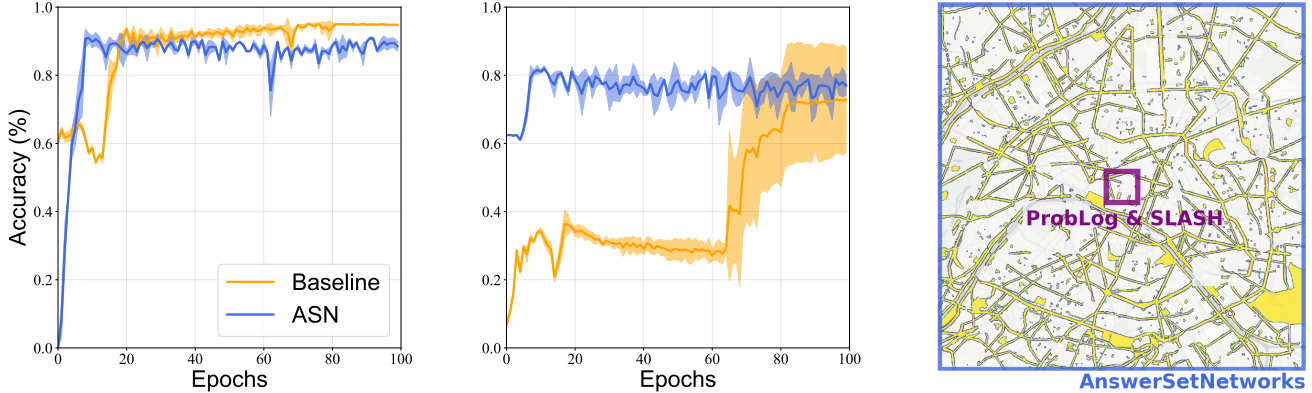
### Q1 LLM Fine-Tuning with ASN

Berglund et al. (2024) have shown in their work that LLMs suffer from the Reversal Curse. Meaning, if a model is trained on a sentence of the form “ $A \Rightarrow B$ ”, it will not automatically generalize to the reverse direction “ $B \Rightarrow A$ ”. To this end, authors tested SOTA LLMs on pairs of questions like “Who is Tom Cruise’s mother?” and “Who is Mary Lee Pfeiffer’s son?”. Here, we demonstrate how ASN allows for abductive reasoning while fine-tuning LLMs to resolve the reversal problem.

To address this issue, we perform *abductive fine-tuning* of the LLM using ASN. Particularly, during training, we predict the relation (mother, father, daughter, and son) between a celebrity and their parent(s) in both directions. The training dataset consists of queries such as “Q: What is the relation between <celebrity\_name> and <celebrity\_parent\_name>? A: ...” and the opposite of the prompt by swapping <celebrity\_name> and <celebrity\_parent\_name>. For each celebrity, we only provide one direction during training, i.e., either child-parent or parent-child. We split the dataset into equal parts for each direction respectively to prevent the fine-tuned model from becoming biased in either direction. During test time, we evaluate the accuracy of unseen celebrities and their parents in both directions.

We add 12M learnable parameters by LoRA (Hu et al. 2021) to fine-tune the Llama2-7B (Touvron et al. 2023) LLM using ASN. To compare the results of ASN fairly, we fine-tuned the Llama2 in a stand-alone fashion as well. The difference in the training procedure is founded in ASN’s ability to derive the opposite relation, while baseline handles only one direction for each celebrity. Using the original dataset from (Berglund et al. 2024), we split the 797 celebrities into 70% train, 20% test, and 10% validation. For in-depth explanations of the experimental setup, we refer our readers to consult the appendix.

The results reveal the following findings. Firstly, ASN’s runtime equates to the number of passes through the LLM. Namely, we request both the sex and the relation for two persons for every query. In particular, the baseline takes 50s and ASN 189s, which corresponds to the four forward passes and one backward. Secondly, ASN converges one order of



(a) **ASN improves LLM’s convergence during fine-tuning:** Learning to answer the query “Q: Relation from Mary Lee Pfeiffer to Tom Cruise? A: Mother.” (left) is easier than “Q: Relation from Tom Cruise to Mary Lee Pfeiffer? A: Son.” (right). Fine-tuning with ASN can significantly enhance convergence by supplying the LLM with the inverse signal, specifically  $B \Rightarrow A$ , derived from  $A \Rightarrow B$ , and vice versa.

(b) **ASN renders Paris in 56m:** Colored areas show where air travel is allowed, zero probability is uncolored. Meanwhile, SLASH & ProbLog render a fraction of the map, shown by the purple square.

Figure 5: ASN on Abductive Fine-Tuning of LLMs and ProMis over Paris during the Olympics.

magnitude faster (in the number of epochs) than the baseline. In detail, Fig. 5a (right) paints the picture for ASN taking only 9 epochs (28m:21s) vs. 96 (80m) for the baseline. On the left, again, there were only 9 (28m:21s) for ASN and 72 (60m) for the baseline. Lastly, ASN beats the baseline in the more complex direction “ $B \Rightarrow A$ ” (82.2% vs 72.8%) and performs slightly worse in the easier direction of “ $A \Rightarrow B$ ” (90.9% vs 95.1%). Regarding **Q1**, these findings confirm the numerous and computationally attractive advantages of abductive fine-tuning of LLMs with ASN, laying a foundation for future advances in guiding LLMs with logic.

## Q2 Mission Design for Unmanned Aerial Vehicles

Logic is crucial to ensure safety constraints, e.g., in autonomous navigation. This is evident when considering autonomous agents navigating in human-inhabited spaces. For example, a complex set of rules must be enforced when considering novel applications of Advanced Aerial Mobility, such as in cutting-edge logistics tasks. Similarly, metropolitan areas and capital cities pose a particular challenge due to their complex infrastructure and large scale. Within their borders, they often contain consulates of numerous countries, government buildings, etc. They can also host major events that attract numerous international guests from all over the world. All of this makes navigation particularly challenging because such events require additional temporary regulations that must be adhered to. At the time of writing, for example, Paris, France’s capital, is the host city for the 2024 Olympic Games. Hence, in this experiment, we show how ASN scales NeSy methods for safe navigation to such large-scale scenarios by densely sampling Paris’ area.

In the ProMis framework (Kohaut et al. 2023), the requirements of public laws and operator preferences are en-

coded in a probabilistic logic language. Essentially, one obtains i.i.d. generative models for each continuous point in the agent’s navigation space. Although one can compute probabilities independently, splitting up work and parameters in a multithreaded setting, a large number of logic programs need to be solved. For each  $(x_i, y_i) \in \mathcal{S}$  of points  $\mathcal{S}$  in a two-dimensional navigation space, we query for a valid  $airspace(x_i, y_i)$ . All models entailed via the constraint that encodes the query fulfill one of the rules defining wherever the UAV is allowed to visit the specified point.

ProMis obtains a probability for each coordinate  $(x_i, y_i)$  via Hybrid ProbLog (Gutmann, Jaeger, and Raedt 2010). Using a stochastic error model (Flade, Kohaut, and Eggert 2021), it converts crowdsourced geographic features from OpenStreetMap into probabilistic facts. These probabilistic facts encode probabilities for spatial relations between coordinates and tagged features, e.g., whether a coordinate is likely over a public park or far away from the nearest sports arena. Note that the probabilities are “hard-coded” as they are obtained from the input map and not forwarded through a neural network, i.e., we use NPPs to encode the probabilities within the ASP program and use SLASH’s inference mechanism without training. Via SLASH, we can then compute the query probability  $p(Q)$  from the stable models, which ASN computes for each coordinate.

To cover the area of 169km<sup>2</sup>, we must solve 6500<sup>2</sup> programs corresponding to all coordinate query pairs. The resulting map can be seen in Fig. 5b. Despite the problem’s size and complexity, ASN successfully generated the visible map in **56m:32s**. We took the time to compute a 500<sup>2</sup> grid for ProbLog and SLASH and multiplied it by 169 to obtain the time it would take to compute the whole grid. For ProbLog, it would take **7d:15h** and **5d:9h** for SLASH.

Method	Accuracy after last Epoch			Average Time per Epoch		
	T1	T2	T3	T1	T2	T3
DeepProbLog	98.50	98.75	98.23	8m:3s	15m:36s	34m:54s
SLASH	98.80	98.85	98.75	24s	1m:42s	51m:49s
SAME	98.56	98.82	98.71	17s	17s	1m:35s
ASN	98.83	98.73	98.47	5s	9s	35s

Table 1: **ASN scales well with growing task complexity:** Test accuracy in % and runtime comparison for MNIST-Addition task. The runtime is averaged over ten epochs and five seeds for all methods. Light green indicates high accuracy or low time, while blue represents the opposite.

This makes ASN 194 and 137 times faster on ProMis than ProbLog and SLASH, respectively. These findings answer **Q2** strongly, and we conclude that ASN’s scalability opens up the opportunity to investigate further related problems. E.g., such as automated route planning (Stenger, Fernando, and Heni 2013) and reactive navigation (Patrinooulou et al. 2023). For further details on hyperparameter tuning of batch-size and other details, we refer to the appendices.

### Q3 MNIST-Addition

In the MNIST-addition task (Manhaeve et al. 2018), the objective is to predict the sum of two images from the MNIST dataset, where the images are provided as raw data. During testing, the model must classify the images directly without explicit information about the digits they depict. Instead, it learns to recognize the digits through indirect feedback on the sum prediction. Handling more than two images significantly increases the task complexity due to the exponential growth in possible digit combinations. Similar to SAME (Skryagin et al. 2023), we assess the model’s scalability across three difficulty levels. These levels range from task T1, depicting two images with a target sum, e.g.  $sum2(3, 7, 10)$ , to task T3, which includes four images depicting digits as in  $sum4(3, 7, 5, 2, 17)$ . We evaluate performance using LeNet5 (LeCun et al. 1998) as a NPP for the same experimental settings.

Following the results in Tab. 1, we observe that ASN is a highly beneficial solver for SLASH (Skryagin et al. 2022). Regardless of the tasks’ complexity, ASN provides the big leap in computational speed, surpassing SAME (Skryagin et al. 2023): T1 is 3,4 times faster, T2 - 1,89, and T3 - 2.71. These results answer **Q3** positively and confirm that seamlessly integrating subsymbolic models for NeSy tasks via ASN should be investigated further. We refer to appendix for an in-depth discussion about choices of batch size, the example of a program, and its RG.

In summary, we have demonstrated in the experimental section how ASN positively impacts NeSy tasks that have to be solved multiple times with different configurations. For these problems, which are at the heart of NeSy AI, the proposed ASN bridge the gap by bringing the symbolic part to the neural part, which lies on the GPU.

## Related Work

### Automated Reasoning

Classic logic programming employs a two-step approach: grounding and solving. Grounding transforms the program into a variable-free representation while solving involves enumerating valid combinations of true and false ground atoms using techniques like the Davis-Putman-Logemann-Loveland (DPLL) algorithm (Davis, Logemann, and Loveland 1962), no-good (Dechter and Meiri 1990) assignments, and conflict-driven (Marques-Silva and Sakallah 1996) methods. Satisfiability Modulo Theories (SMT) generalize the setting, capturing full ASP semantics. Popular ASP solvers include clingo (Gebser et al. 2011) and DLV (Alviano et al. 2017). Although the field of SAT and SMT solvers is competitive and consistently improves at solving complex problems (Fazekas, Bacchus, and Biere 2018), single-core execution inherently limits their potential (Heule, Kullmann, and Marek 2015) for NeSy applications. In contrast, Answer Set Networks achieve state-of-the-art performance on these tasks as GPU-accelerated ASP solvers.

### Probabilistic Logic Programming

Probabilistic inference over a model’s potential solutions is necessary to capture ambiguities in the modeled problem. This is the case in Visual Question Answering problems (Antol et al. 2015), with various datasets and benchmarks emerging (Marino et al. 2019; Schwenk et al. 2022; Johnson et al. 2017; Nerdimite 2022). Probabilistic logic languages, like ProbLog (Fierens et al. 2015), propose Weighted (Sang, Beame, and Kautz 2005) and Algebraic Model Counting (Kimmig, Van den Broeck, and De Raedt 2017) over a foundation of SAT-based Prolog. As these systems depend on automated reasoning, as discussed above, the performance gains of ASN directly translate to probabilistic logic languages.

### Neural-Symbolic Systems

The NeSy approach combines neural and symbolic methods, leveraging their complementary strengths. For instance, DeepProbLog (Manhaeve et al. 2018) and Scallop (Huang et al. 2021) extend the semantics of ProbLog with Neural Predicates that encapsulate neural networks, e.g., to integrate image perception into probabilistic logic. ASP-based systems like SLASH (Skryagin et al. 2022) and NeurASP (Yang, Ishay, and Lee 2020) have been presented. But, all of the above suffer the issue of dominating computation time for symbolic computation. In this work, we relate to ASP-based NeSy system, intertwining neural reasoning with symbolic modeling in ASP and enabling scalability to larger problems.

## Conclusions and Future Work

We have presented Answer Set Networks (ASN), a novel neural-symbolic (NeSy) solver for Answer Set Programs (ASP) using Reasoning Graphs (RG). To illustrate the advantages of ASN, we evaluated its capabilities on various NeSy tasks. To the best of our knowledge, we are the first to

fine-tune large language models (LLMs) within deep probabilistic programming languages (DPPLs).

Through Answer Set Networks, we have made considerable steps towards a vast world of future applications of NeSy AI systems. Hereby, ASNs allow for distributed graph learning, allowing the symbolic component to be scaled alongside the neural component to larger problems and datasets. Future developments could focus on optimizing the definitization and readout processes, possibly exploring techniques to mitigate the higher memory-print associated with increasing choices while maintaining compatibility with its main goal of integration with sub-symbolic models. Further, thanks to GNNs being the backbone of RG, the next natural step will be to realize differentiable weighted-model semantics for ASN.

## A - Experimental Details

### LLM Fine-Tuning

**Training Setup** – For training, we ask the following query: “What is the relation between <person1> and <person2>? The answer is:”. We then predict the next token and obtain the logits for the four relation classes: mother, father, daughter and son. There are two directions we are interested in:

- **parent-child:** “What is the relation between <celeb\_parent\_name> and <celebrity\_name>? The answer is:”  $\Rightarrow$  mother or father
- **child-parent:** “What is the relation between <celebrity\_name> and <celeb\_parent\_name>? The answer is:”  $\Rightarrow$  daughter or son

(Berglund et al. 2024) provided the dataset consisting of 797 unique celebrity names, 81 of which have only one parent in the dataset and 716 with two parents in the dataset. This results in  $81 + 716 * 2 = 1513$  parent-child and additional reversed, 1513 child-parent relations in total.

For training, we provide the model with both directions but will never give them both directions for a single celebrity. If the model sees Tom Cruise and Mary Lee Pfeiffer in that order, it will never see Mary Lee Pfeiffer and Tom Cruise in that order.

**Data splits:** We split up the unique celebrity names into 70% for training, 20% for testing, and 10% for the validation dataset. From 557 unique celebrity names drawn at random for training, we obtain 1054 parent-child combinations as we have on average slightly less than two parents. Next, we randomly split them into 50% child-parent and 50% parent-child pairs.

Similarly, the test and validation datasets are built, but we keep them separate as shown in Fig. 5a.

**Logic Program:** While the baseline will only get a training signal from the data points in one direction, ASN will infer the relation from the other direction using the program in Listing 1. To infer if the reverse relation is mother or father for parent-child relations or daughter or son for child-parent relations, the sex of the second person is required. For this, the program encodes a call to the LLM that returns the probability for sex. This way, we don’t need to provide the data ourselves but can leverage the knowledge stored in the LLM itself.

BS	25	50	250	500	2.5k	5k	25k	50k	250k
Time	7m:21s	3m:41s	1m:2s	42s	27s	24s	22s	22s	21s

Table 2: **Batching ProMis with ASN:** Runtime comparison to compute a  $500^2$  grid with different batch sizes in ASN. Increasing the batch steadily reduces the computation time.

Batch Size	Total Time (#Epochs)					
	T1 time	e	T2 time	e	T3 time	e
64	1m:20s	(2)	6m:51s	(2)	1h:1m:13s	(2)
128	0m:45s	(2)	3m:36s	(2)	47m:5s	(3)
256	0m:26s	(2)	2m:46s	(3)	24m:10s	(3)
512	0m:24s	(3)	1m:59s	(4)	21m:10s	(5)
1024	<b>0m:22s</b>	(4)	1m:35s	(6)	17m:11s	(8)
2048	0m:31s	(7)	<b>1m:32s</b>	(10)	16m:54s	(15)
4096	0m:46s	(12)	1m:59s	(19)	<b>15m:51s</b>	(27)
8192	1m:23s	(23)	2m:53s	(38)	15m:46s	(50*)
15000	2m:50s	(49)	3m:8s	(48)	9m:3s	(50*)

\* Did not reach the accuracy threshold within the maximum number of epochs.

Table 3: **Batch size trade-off for MNIST-addition:** Models were trained for a maximum of fifty epochs to achieve a competitive accuracy of  $\geq 98\%$ . Results for 30k are not shown as they did not converge in 50 epochs, and the dataset size for T2 and T3 is 20k and 15k, respectively.

### ProMis

In ASN, ProbLog, and SLASH, we must solve  $6500^2$  programs corresponding to all coordinate query pairs to render Paris with each point corresponding to  $2m^2$ . Due to the graph-based nature, ASN can batch multiple queries together for parallel computation on the GPU, as described at the end of Sec. Consequently, we first want to evaluate the effect of batching in ASN by comparing increasing batch sizes. Table 2 shows the impact of different batch sizes on the time it takes to compute a grid with a resolution of  $500^2$ . We observe that batching is an effective strategy to speed up the computation. After reaching a certain batch size, further gains are only marginal. For the ProMis Paris experiment, we used a high batch size of  $500^2$ .

While in ASN, we can use batching to speed up the compute time, we can group multiple coordinates together in one ProbLog program as in (Kohaut et al. 2023). We found that using 16 coordinates per program resulted in the fastest time and used it to compare with ASN. For SLASH we can use multiple CPU’s in parallel and found 20 CPUs to be the fastest.

### MNIST-Addition

**Computation of Batch Size** – Having seen the scaling abilities of ASN for ProMis, it is beneficial to address how a chosen batch size influences both the resulting accuracy and the number of epochs until the convergence point. Tab. 3 shows the total training time (average time per epoch multiplied by the average number of trained epochs to reach a threshold of 98%). The numbers in parentheses after the reported times indicate the number of epochs needed. Note that for T1 and a batch size of 30k, all runs did not meet the

accuracy criteria within the maximum number of epochs. Furthermore, for T2 and T3, the data sets contain a maximum of 20k and 15k training points, respectively, which is why the largest batch size we report is 15k.

Following the results, we see a non-obvious optimum for every complexity level. The bigger the batch size, the faster it is to train for one epoch. As neural network training is involved in this experiment, we cannot simply choose the largest batch size to lower compute time, as in ProMis: The higher the batch size, the longer it takes the network to converge. Consequentially, for every task, it is necessary to tune the batch size to achieve the maximum speed-up without compromising the overall accuracy.

**Computation Speed** – After seeing the influence of choosing the batch size, let us look at what happens if we compare the average time per epoch following the setting proposed in (Skryagin et al. 2023). Therefore, we use Deep-ProbLog (Manhaeve et al. 2018), SLASH, and SAME as baselines. Having reimplemented SLASH with ASN, we thus have a fair comparison. Tab. 1 lists the results showing ASN scalability advantages. It tightly binds the end-to-end computations for WMC (Sang, Beame, and Kautz 2005) in a differentiable way so that even SAME dynamically pruning the potential solutions is not keeping pace. Thereby, it is noticeable that the bigger the solution space of the task at hand, the greater the speed-up ASN allows. As a result, we argue that ASN paves the way for vastly complex and, until now, only cumbersome solvable tasks in NeSy AI.

## B - Programs

Here, the interested reader will find the ASP programs which we compiled for our ablation studies on abductive fine-tuning, ProMis over Paris and MNIST-addition.

**LLM Fine-Tuning with ASN** Listing 1 shows the SLASH program used for the task, and Fig. 7 outlines its RG.

**ProMis** Listing 2 shows the simplified version of the source code, and Fig. 8 offers its RG.

**MNIST-Addition** Listing 3 lists the source code for the task, while Fig. 9 shows the according RG.

Listing 1: Abductive fine-tuning of LLM to alleviate the “Reversal Curse”

---

```

1  % We use the same LLM playing the role
    of both NPPs. I.e., two forward
    passes to obtain the probabilities.
2  person(p1). person(p2).
3
4  % NPP to determine the relation of two
    different persons
5  #npp(relation(X1,X2),[mother, father,
    daughter, son]) :- person(X1),
    person(X2), X1 != X2.
6
7  % NPP to determine the sex of a person
8  #npp(sex(X),[male, female]) :-
    person(X).
9
10 % Exclude sexes being open.
11 :- relation(X1,X2,mother), sex(X1,male).
12 :- relation(X1,X2,father),
    sex(X1,female).
13 :- relation(X1,X2,son), sex(X1,female).
14 :- relation(X1,X2,daughter),
    sex(X1,male).
15
16 % Constraining relations to be acyclic.
17 :- relation(X1,X2,daughter),
    relation(X2,X1,son).
18 :- relation(X1,X2,son),
    relation(X2,X1,son).
19 :- relation(X1,X2,daughter),
    relation(X2,X1,daughter).
20
21 % Constraining possible relations
22 % C1: If the child is male, than it is
    a son.
23 relation(X2,X1,son) :-
    relation(X1,X2,mother), sex(X2,male).
24 relation(X2,X1,son) :-
    relation(X1,X2,father), sex(X2,male).
25
26 % C2: If the child is female than it is
    a daughter
27 relation(X2,X1,daughter) :-
    relation(X1,X2,mother),
    sex(X2,female).
28 relation(X2,X1,daughter) :-
    relation(X1,X2,father),
    sex(X2,female).
29
30 % Query
31 :- not relation(p1,p2,daughter).
32 :- not relation(p1,p2,son).
33 :- not relation(p1,p2,mother).
34 :- not relation(p1,p2,father).

```

---



## AnswerSetNetworks

Figure 6: Visualization ProMis Paris in full size

---

Listing 2: ProMis over Paris ASP-program. Only one query included for illustration.

---

```
1 % Single pixel defined by latitude and
  longitude as tuple (x,y)
2 point(x0,y0).
3
4 % Batch of probabilistic facts
5 #npp(over(X,Y,park), [1,0]):-
  point(X,Y).
6 #npp(over(X,Y,primary), [1,0]):-
  point(X,Y).
7 #npp(over(X,Y,eiffel_tower_stadium),
  [1,0]):- point(X,Y).
8 #npp(over(X,Y,bercy_arena), [1,0]):-
  point(X,Y).
9 #npp(over(X,Y,secondary), [1,0]):-
  point(X,Y).
10 #npp(embassy(X,Y), [1,0]):- point(X,Y).
11 #npp(government(X,Y), [1,0]):-
  point(X,Y).
12
13 % Its okay to go over park areas
14 permission(X,Y) :- over(X,Y, park, 1).
15
16 % Its okay to fly over major roads
17 permission(X,Y) :- over(X, Y,
  primary,1).
18 permission(X,Y) :- over(X, Y,
  secondary,1).
19
20 % Define sport sites
21 sport_sites(X,Y) :- over(X,Y,
  eiffel_tower_stadium,0).
22 sport_sites(X,Y) :- over(X,Y,
  bercy_arena,0).
23
24 % Define public buildings
25 public_building(X,Y) :- embassy(X,Y,0).
26 public_building(X,Y) :-
  government(X,Y,0).
27
28 % It is not allowed to fly over sport
  sites and public buildings
29 permitted(X,Y) :- sport_sites(X,Y).
30 permitted(X,Y) :- public_building(X,Y).
31
32 % We are only permitted to fly over the
  permitted areas which are not
  restricted otherwise
33 airspace(X,Y) :- permission(X,Y), not
  permitted(X,Y).
34
35 % Query
36 :- not airspace(x0, y0).
```

---

---

Listing 3: MNIST Addition ASP-program. Every image is either a zero, a one or a two. Queries are just an example of potential outcomes of addition.

---

```
1 % Both images are facts of the program
2 img(i1). img(i2).
3
4 % NPP-rule
5 #npp(digit(X), [0,1,2]) :- img(X).
6
7 % Addition
8 addition(A,B,N1+N2) :- digit(A,N1),
  digit(B,N2), A<B.
9
10 % Exclude symmetries
11 addition(A,B,N) :- addition(A,B,N), A<B.
12
13 % Queries
14 :- not addition(i1,i2,0).
15 :- not addition(i1,i2,1).
16 :- not addition(i1,i2,2).
17 :- not addition(i1,i2,3).
18 :- not addition(i1,i2,4).
```

---

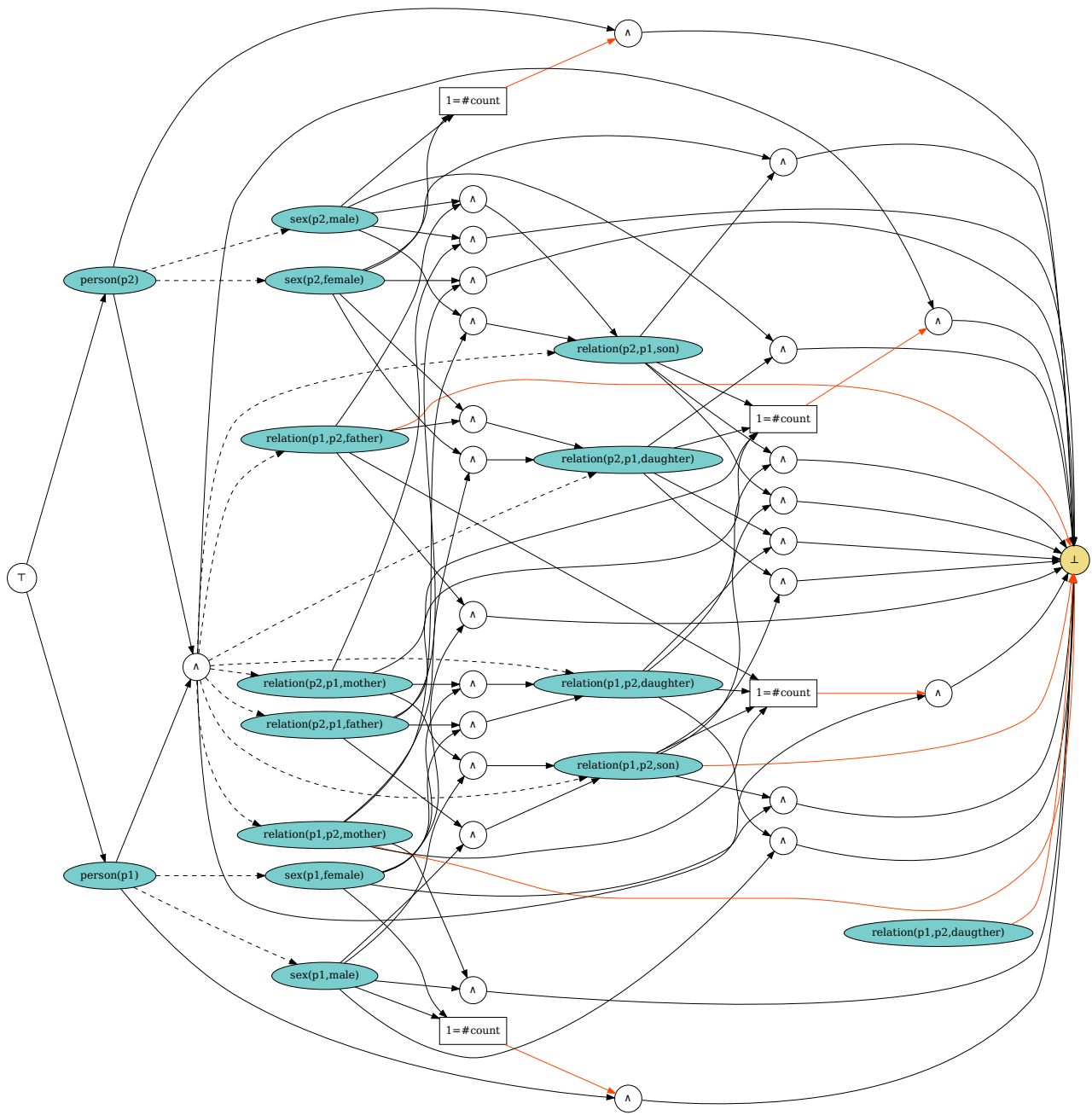


Figure 7: **Reasoning Graph for LLM Fine-Tuning with ASN:** We query for all four possible relationship types among two persons and pick the one with the highest probability.

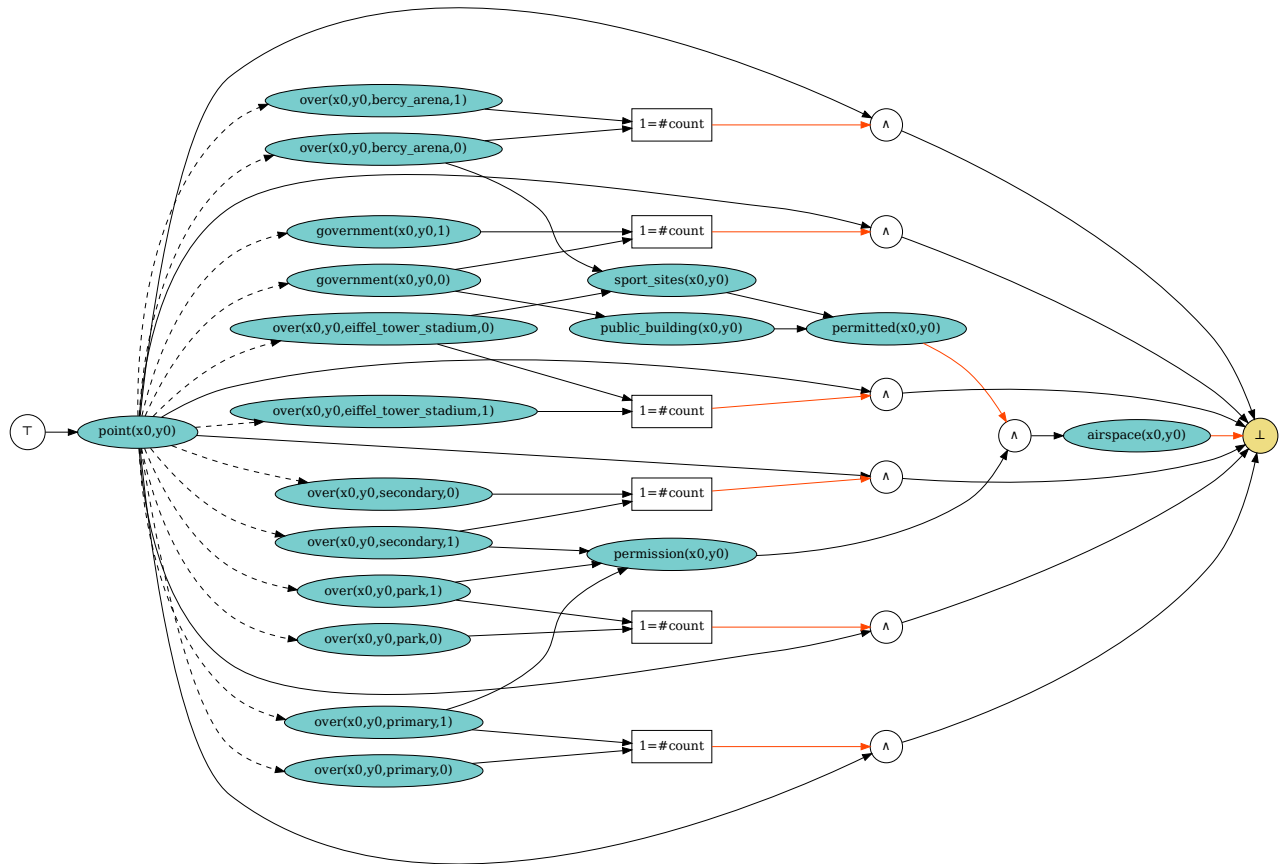


Figure 8: *Reasoning Graph for ProMis on Paris*: Only one grid point is listed as query for the RG to become easily displayable.

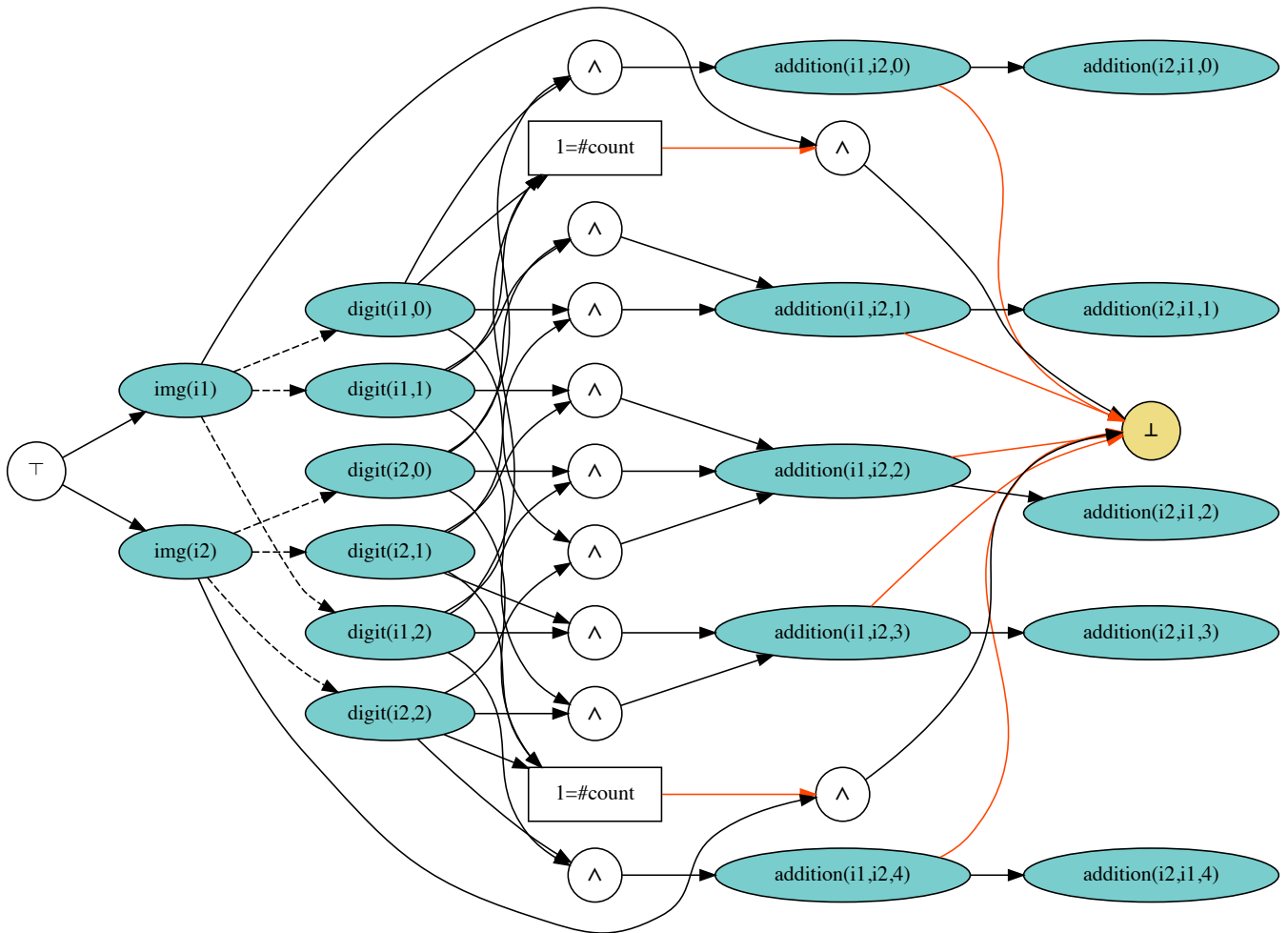


Figure 9: **Reasoning Graph for MNIST-Addition:** The number of classes was restricted to  $[0, 1, 2]$  for the RG to become easily displayable.

## References

- Alviano, M.; Calimeri, F.; Dodaro, C.; Fuscà, D.; Leone, N.; Perri, S.; Ricca, F.; Veltri, P.; and Zangari, J. 2017. The ASP System DLV2. In *Logic Programming and Nonmonotonic Reasoning*.
- Antol, S.; Agrawal, A.; Lu, J.; Mitchell, M.; Batra, D.; Lawrence Zitnick, C.; and Parikh, D. 2015. VQA: Visual Question Answering. *CVPR*.
- Berglund, L.; Tong, M.; Kaufmann, M.; Balesni, M.; Stickland, A. C.; Korbak, T.; and Evans, O. 2024. The Reversal Curse: LLMs trained on “A is B” fail to learn “B is A”. arXiv:2309.12288.
- Calimeri, F.; Faber, W.; Gebser, M.; Ianni, G.; Kaminski, R.; Krennwallner, T.; Leone, N.; Maratea, M.; Ricca, F.; and Schaub, T. 2020. ASP-Core-2 Input Language Format. *Theory and Practice of Logic Programming*, 20: 294–309.
- Choi, Y.; Vergari, A.; and Van den Broeck, G. 2020. Probabilistic Circuits: A Unifying Framework for Tractable Probabilistic Models. In *AAAI*.
- Darwiche, A. 2011. SDD: A New Canonical Representation of Propositional Knowledge Bases. In *IJCAI*.
- Davis, M.; Logemann, G.; and Loveland, D. 1962. A machine program for theorem-proving. *Communications of the ACM*.
- Dechter, R.; and Meiri, I. 1990. Network-based heuristics for constraint-satisfaction problems. *Artificial Intelligence*.
- Fazekas, K.; Bacchus, F.; and Biere, A. 2018. Implicit Hitting Set Algorithms for Maximum Satisfiability Modulo Theories. *IJCAR*.
- Fierens, D.; den Broeck, G. V.; Renkens, J.; Shterionov, D. S.; Gutmann, B.; Thon, I.; Janssens, G.; and Raedt, L. D. 2015. Inference and learning in probabilistic logic programs using weighted Boolean formulas. *Theory Pract. Log. Program.*, 15(3): 358–401.
- Flade, B.; Kohaut, S.; and Eggert, J. 2021. Error Decomposition for Hybrid Localization Systems. In *2021 IEEE International Intelligent Transportation Systems Conference (ITSC)*, 149–156. IEEE.
- Gebser, M.; Kaufmann, B.; Kaminski, R.; Ostrowski, M.; Schaub, T.; and Schneider, M. 2011. Potassco: The Potsdam Answer Set Solving Collection. *AI Communications*.
- Gutmann, B.; Jaeger, M.; and Raedt, L. D. 2010. Extending ProbLog with Continuous Distributions. In *Inductive Logic Programming - 20th International Conference, ILP 2010, Florence, Italy, June 27-30, 2010. Revised Papers*, volume 6489 of *Lecture Notes in Computer Science*, 76–91. Springer.
- Heule, M. J.; Kullmann, O.; and Marek, V. W. 2015. Solving and Verifying the Boolean Pythagorean Triples Problem via Cube-and-Conquer. *SAT*.
- Hu, E. J.; Shen, Y.; Wallis, P.; Allen-Zhu, Z.; Li, Y.; Wang, S.; Wang, L.; and Chen, W. 2021. LoRA: Low-Rank Adaptation of Large Language Models. arXiv:2106.09685.
- Huang, J.; Li, Z.; Chen, B.; Samel, K.; Naik, M.; Song, L.; and Si, X. 2021. Scallop: From Probabilistic Deductive Databases to Scalable Differentiable Reasoning. In *Advances in Neural Information Processing Systems 34: Annual Conference on Neural Information Processing Systems*.
- Johnson, J.; Hariharan, B.; van der Maaten, L.; Fei-Fei, L.; Lawrence Zitnick, C.; and Girshick, R. 2017. CLEVR: A Diagnostic Dataset for Compositional Language and Elementary Visual Reasoning. *CVPR*.
- Kimmig, A.; Van den Broeck, G.; and De Raedt, L. 2017. Algebraic model counting. *Journal of Applied Logic*.
- Kohaut, S.; Flade, B.; Dhimi, D. S.; Eggert, J.; and Kersting, K. 2023. Mission Design for Unmanned Aerial Vehicles using Hybrid Probabilistic Logic Programs. In *26th IEEE International Intelligent Transportation Systems Conference (ITSC)*.
- LeCun, Y.; Bottou, L.; Bengio, Y.; and Haffner, P. 1998. Gradient-based learning applied to document recognition. *Proceedings of the IEEE*, 86: 2278–2324.
- Li, F. 2021. Graph Based Answer Set Programming Solver Systems. In *Proceedings 37th International Conference on Logic Programming (Technical Communications), ICLP Technical Communications 2021, Porto (virtual event), 20-27th September 2021*, 276–285.
- Manhaeve, R.; Dumancic, S.; Kimmig, A.; Demeester, T.; and Raedt, L. D. 2018. DeepProbLog: Neural Probabilistic Logic Programming. In *Advances in Neural Information Processing Systems 31: Annual Conference on Neural Information Processing Systems*.
- Marino, K.; Rastegari, M.; Farhadi, A.; and Mottaghi, R. 2019. OK-VQA: A Visual Question Answering Benchmark Requiring External Knowledge. *CVPR*.
- Marques-Silva, J. P.; and Sakallah, K. A. 1996. GRASP—a new search algorithm for satisfiability. In *ICCAD*.
- Nerdimite. 2022. Neuro-Symbolic AI for Visual Question Answering. *GitHub Repository*.
- Patrinopoulou, N.; Lappas, V.; Daramouskas, I.; Meimētis, D.; and Kostopoulos, V. 2023. Autonomy in UAV Civilian Applications. In *Autonomous Vehicles*. IntechOpen.
- Sang, T.; Beame, P.; and Kautz, H. 2005. Performing Bayesian inference by weighted model counting. *NCAI*.
- Schwenk, D.; Khandelwal, A.; Clark, C.; Marino, K.; and Mottaghi, R. 2022. A-OKVQA: A Benchmark for Visual Question Answering Using World Knowledge. *CVPR*.
- Skryagin, A.; Ochs, D.; Singh Dhimi, D.; and Kersting, K. 2023. Scalable Neural-Probabilistic Answer Set Programming. In *Journal of Artificial Intelligence Research*, volume 78, 579–617.
- Skryagin, A.; Stammer, W.; Ochs, D.; Dhimi, D. S.; and Kersting, K. 2022. Neural-Probabilistic Answer Set Programming. In *Proceedings of the 19th International Conference on Principles of Knowledge Representation and Reasoning*.
- Stenger, A.; Fernando, B.; and Heni, M. 2013. Route Planning for Unmanned Aerial Vehicles. *Deutscher Luft- und Raumfahrtkongress*.

Touvron, H.; Martin, L.; Stone, K.; Albert, P.; Almahairi, A.; Babaei, Y.; Bashlykov, N.; Batra, S.; Bhargava, P.; Bhosale, S.; Bikel, D.; Blecher, L.; Canton, C.; Chen, M.; Cucurull, G.; Esiobu, D.; Fernandes, J.; Fu, J.; Fu, W.; Fuller, B.; Gao, C.; Goswami, V.; Goyal, N.; Hartshorn, A.; Hosseini, S.; Hou, R.; Inan, H.; Kardaş, M.; Kerkez, V.; Khabsa, M.; Kloumann, I.; Korenev, A.; Singh, P.; Lachaux, M.-A.; Lavril, T.; Lee, J.; Liskovich, D.; Lu, Y.; Mao, Y.; Martinet, X.; Mihaylov, T.; Mishra, P.; Molybog, I.; Nie, Y.; Poulton, A.; Reizenstein, J.; Rungta, R.; Saladi, K.; Schelten, A.; Silva, R.; Michael, E.; Subramanian, R.; Ellen, X.; Tang, B.; Taylor, R.; Williams, A.; Xiang, J.; Xu, P.; Yan, Z.; Zarov, I.; Zhang, Y.; Fan, A.; Kambadur, M.; Narang, S.; Rodriguez, A.; Stojnic, R.; Edunov, S.; and Scialom, T. 2023. Llama 2: Open Foundation and Fine-Tuned Chat Models. arXiv:2307.09288.

Trinh, T. H.; Wu, Y.; Le, Q. V.; He, H.; and Luong, T. 2024. AlphaGeometry: Solving Olympiad Geometry without Human Demonstrations. *Nature*.

Yang, Z.; Ishay, A.; and Lee, J. 2020. NeurASP: Embracing Neural Networks into Answer Set Programming. In *Proceedings of the Twenty-Ninth International Joint Conference on Artificial Intelligence*.